Published by :
http://www.ijert.org

International Journal of Engineering Research & Technology (IJERT)
ISSN: 2278-0181
Vol. 5 Issue 03, March-2016

Low Melting Glass Frit as an Adhesion and Resistivity Promotor: Photonically Sintered Silver Nanoparticle Ink on Indium Tin Oxide Coated Glass

Jason Karabin Kleiner, Michael Joyce, Thomas Joyce
Western Michigan University
Department of Paper and Chemical Engineering
Kalamazoo, MI U.S.A

***Abstract*— The objective of this study was the fabrication of a printed circuit resulting from the photonic drying/sintering of conductive circuits, printed using silver nano ink layered on a film of low melting glass frit onto indium tin oxide (ITO) coated glass substrate through the flexographic printing method. The fabrication process flow included material preparation, printing, and photonic drying/sintering in that order.**

Investigation of the breakthrough photonic drying/sintering method was studied by varying process parameters, specifically the amount of heat energy applied to each specimen, and the speed at which it was applied. Additionally, the adhesion promoting properties of a never before studied glass frit was investigated. Their effects were studied by quantifying adhesion and resistivity of the printed film. Adhesion was quantified by mechanically applying abrasive forces, and resistance was measured through the use of a four point collinear probe.

Adhesion improved with an increase in energy flux, and presence of frit, for which both factors were statistically significant. Adhesion decreased with an increase in sintering speed. Resistivity decreased dramatically with an increase in energy flux applied and presences of the adhesion promoter had no significant effect. A clear trend for resistivity as a function of sintering speed could not be observed.

Keywords—Nano Silver Ink, Photonic, Prited Electronics, Indium Tin Oxide, Adhesion, Surface Resistance, Image Analysis.

I. INTRODUCTION

An emerging $300 billion market is expected to be nurtured through the combination of microelectronics, chemistry, and printing, to form an industry known as printed electronics (PE). Industrial and consumer applications are expected in the automotive, building and architecture, chemical, medical, consumer electronics, packaging, and energy industries [1].

The benefits of PE are realized in both industrial products and processes. The breakthroughs within PE will create thin, light weight, potentially wearable electronics that could not previously be achieved. PE will eventually offer manufacturers a means to cost-effectively mass produced products at affordable prices by reducing production and material costs. Silicon technology requires large investments, both in establishment of a production facility and cost per piece. PE requires one-tenth to one-one hundredth of the investment as for an equivalent silicon based manufacturing facility [2].

Applications of PE, such as printed wiring boards have been around since the 1950's, but additive PE did not emerge as the ultimate solution [2]. Complications result from the additive printing processes that effect product quality. One example is the large footprint and long cycle time needed to densify conductive metallic nanoparticles contained in the PE inks with conventional curing furnaces [1]. Densification, or reducing the occupied volume given a particular mass of metallic nanoparticles contained within the ink, allows for an increase in conductivity. Conductivity increases as a result of increased surface area contact of the conductive particles. Breakthroughs for this concern include recently developed methods of densification through the use of photonic sintering. One additional concern is the adhesion of printed circuit inks on exceptionally smooth surfaces, such as glass and finely coated glass. Breakthrough adhesion promoters, such as materials with like chemistries similar to the substrate, may be the answer. No research has been performed on the marriage of these countermeasures to the aforementioned concerns.

The objective of this study was the fabrication of a printed circuit resulting from the photonic sintering of conductive circuits, printed using silver nano ink layered on a film of low melting glass frit onto ITO coated glass substrate through the flexographic printing method. In addition to fabrication of the aforementioned circuit, an investigation of the relative adhesion and resistivity was performed. Adhesion was quantified by an abrasion test and resistance was measured through the use of a four point collinear probe.

II. EXPERIMENTAL

The fabrication and qualification process is comprised of A.) material preparation, B.) printing C.) photonic curing (a.k.a. sintering), and D.) two types of quality tests. Fig. 1 illustrates the process flow from beginning to end. An explanation of the design of experiment (DOE) used for the quality tests will be provided prior to describing the quality testing.

International Journal of Engineering Research & Technology (IJERT)
ISSN: 2278-0181
Vol. 5 Issue 03, March-2016

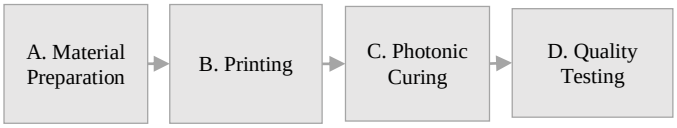

Fig. 1. Process Flow for Fabrication and Qualification of Printed Conductive Film.

A. Suface Preparation

Cleaning is essential and a common step performed when attempting to print on coated glass. A common method of cleaning glass in an industrial setting is a three consecutive bath system, consisting of trichloroethylene, acetone, and isopropyl alcohol in that order. This sequential cleaning has been used successfully by the electronics industry for many years [3].

Trichloroethylene (TCE) is a halogenated alkene, and has been long recognized by a number of different industries for its cleaning power. TCE is a dense substance (1.46 kg/L) with a high vapor density that allows for relatively easy recovery from vapor degreasing systems. It dissolves soils faster, resulting in a cleaner substrate, and provides high output of cleaned glass per unit time [4]. TCE leaves a trace residue when dried, therefore acetone is used to clean further. Similarly to TCE, the acetone also leaves a residue, and, likewise, isopropyl alcohol is used to remove the trace acetone. Isopropyl alcohol, with its low vapor pressure will evaporate, leaving insignificant trace on the glass.

The bath dimensions were such that the substrate would sit flat, and unobstructed by the edges of the container. This measure was taken to ensure that the entirety of the print-side surface, defined as the side of the substrate that the printed film would adhere to, could be covered by the same amount of cleaning agent. The specimen sitting flat would also allow for minimization of stresses, which could create the potential of breakage.

The amount of cleaning agent added to each bath was a volume of 500 mL, chosen to completely submerge the specimen. The bath containers used were sized to fit 5 plates side by side. The number of plates per bath was limited to 5. With a standard volume of cleaning agent above the surface of each plate sitting flat to the horizontal, and a limit to the number of plates per bath, saturation of the cleaning agent with foreign substances was assumed negligible. The plates were submerged for 5 minutes per bath.

B. Printing

Printing is a multifaceted process in which materials such as ink and substrate undergo physical changes in order to produce the end product, repeatability. Printing can be done with a variety of different printing methods and materials, and is selected based on the desired properties of the product. Depending on the nature of the PE product, considerations for ink, specialized additives to the ink, substrate, and print method must be taken.

The ink used throughout the experiment was PFI-722 Silver Flexographic Ink, purchased from Novacentrix, Austin, TX. PFI-722 is intended to be used for printed electronic applications. PFI-722 is a water based ink containing 60% by weight silver nanoparticles (CAS No. 7440-2-4). The ink also contains 1-5% and 2% proprietary adhesive and proprietary rheology additive respectively. The remaining component in the ink is water.

The work of Jang, et al. (2008) describes microstructural evolutions during the annealing process of silver nano ink with and without glass frit applied to a glass substrate by means of ink-jet printing, and annealing at high temperatures (> 400°C). The microstructures were considerably different for films with and without nanometer sized glass frit. The addition of the glass frit was shown to be beneficial to the overall adhesion of the film by way of grain growth. Grain growth is defined as the process of initially small grains melting together to form larger grains of silver and glass frit. Microstructural features found at the level of the film clearly suggest that the glass frit melts to form a liquid phase when the annealing is performed above the glass transition temperature. The liquid glass can effectively fill inter-granular pores between both silver nano particles and the glass substrate. The melting of the glass frit also induces a capillary stress that densifies the film via grain growth. The grains are readily rearranged in the presence of the liquid phase, accommodating large volumetric shrinkage and resulting in a crack-free, smooth, and dense film [5].

In 2012 Hitachi, Ltd. and Hitachi Chemical Co., Ltd. developed a low melting glass frit, able to melt in the range of 220-300 °C, called VS1307. This would act as the adhesion promoter under study. VS1307 contains 40-60% glass frit (CAS No. 65997-17-3), 15-25% Ceramic (CAS No. 66402-68-4),1-5% ethyl cellulose (CAS No. 904-57-3), 1-10% 2-phenoxyethanol (CAS No. 122-99-6) and 40-60 % terpineol (CAS No. 8000-41-7) [6].

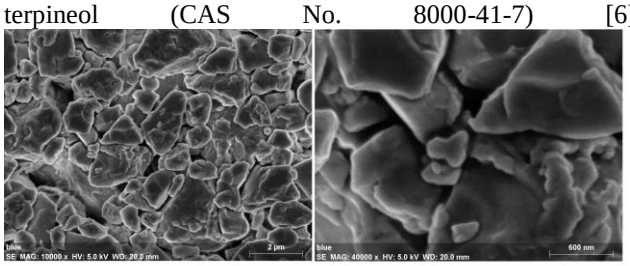

Fig.2 A-B is an image of VS1307 at different magnification, captured from a scanning electron microscope. From the image, the all solids contained within the VS1307 are cuboidal.

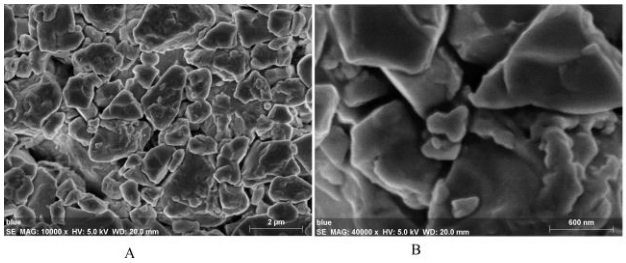

Fig.2. Scanning Electron Microscope Images of VS1307 at Different Magnification, Courtesy of Western Michigan University Chemistry Department. Figure A is 2 micron scale, and B is 600 nm scale.

International Journal of Engineering Research & Technology (IJERT)
ISSN: 2278-0181
Vol. 5 Issue 03, March-2016

The viscosity of the VS1307 of the aforementioned compositions was too viscous to print using the chosen print method, thus additional terpineol was added to the VS1307 mixture in order to allow for adequate printing. The mass composition of the mixture of VS1307 and additional terpineol was 55% VS1307 and 45% terpineol, making the composition of glass frit approximately 27.5 – 33 % glass frit by weight.

The printing method used throughout the study was flexography (flexo). Flexo is a printing process currently used in many industrial applications. While screen printing dominates the PE industry today, flexo accounts for approximately 5% of industrial PE applications [7]. With speeds comparable to a rotary screen (500 m/min) print station, ease of scalability and a capability of producing ink film thicknesses of less than 10 µm, flexo was a suitable candidate for study in this research.

The choice of substrate was ITO coated glass obtained from Gentex Inc., Zeeland, MI. The glass measured 100 by 110 by 1.5 mm, and only one side is coated with the ITO. ITO coated glass is an attractive, transparent electrode used widely for displays, photovoltaics, flat panel displays, lightings, electrochromic windows, and many other optoelectronic devices. Presently, ITO is commercially the most popular transparent conductor due to its low resistivity (approximately 1 x 10^{-4} Ω cm) and high optical transmittance (85%) [8].

The printing press used was a QD Phantom Flexographic Proofing press, developed by Harper Scientific, Charlotte, NC. The proofing press is designed to be used for laboratory scale use. The printing press is comprised of three main components, the press bed, the carriage assemble, and the variable speed carriage rail mechanism. The press bed is the rest fixture for substrate on which the printed film is applied. The press bed provides force on the substrate in the opposite direction as the carriage assembly, allowing the ink to transfer from the carriage assembly to the substrate. The carriage assembly,

Fig. 3, is made up of the carriage, transfer roller, anilox roll, and the doctor blade. It is this assembly that works as the flexo printing systems [9]. The minimal utilities needed also make the press portable.

Constants for the DOE included the carriage assembly utilized a non-image transfer roll, 2.57 billion cubic micron cell volume anilox, springs applying the pressure to the carriage assembly (spring constant = 13kg/m), and the speed (3.4 m/min).

The ink used was removed from the cold storage 30 minutes prior to printing. Printing was done per Harper Scientific instruction. Printing of the thin film consisting of individual layers of either the PFI-722 and/or modified VS1307 mixture.

Printing was completed layer by layer after a partial drying time. Each layer beneath the top layer was printed and allowed to partially dry for 1 day before printing each additional layer in a climate controlled room kept at 23 °C and 60% relative humidity. This partial drying allowed the bottom layer to remain intact whilst the additional layer was printed. Once all layers were present, the specimen was immediately subjected to the photonic curing process.

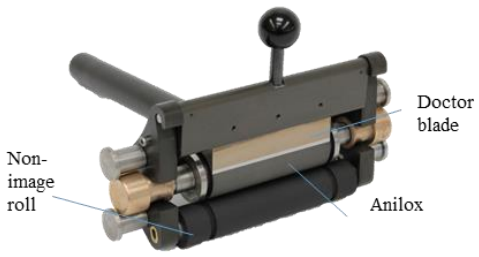

Fig. 3. Harper Scientific Carriage Assembly with Rubber Transfer Roll [8].

C. *Photonic Curing*

Drying is the process in which energy is added to the substrate/ink system in order to evaporate the solvent contained within the ink. Evaporation of the solvent allows for densification of the ink into a film, comprised from the ink's solids remaining on the substrate. These solids are electrically conductive, and what allows for the working circuit. If the energy applied during the drying step is sufficient enough that the particles will melt into a solid layer, sintering occurs. Sintering increases the particle's area of contact and consequently increases conductivity. The increase of conductivity is desirable when designing PE utilizing relatively small voltage potentials.

The bottle neck of most PE processes is the drying process, which typically requires more than 30 minutes and elevated temperatures (250 °C) for the metal particles in the ink to densify. If a web speed of 1 m/s is considered, the long sintering time makes roll-to-roll production very cost ineffective due to the necessary overall length of the line [1], [10]. Compensating with an increase in temperature can be unfeasible, as it introduces a condition in which the ink's solvent vaporizes too fast causing a "sputtering" effect, creating voids and discontinuity in the film, ultimately resulting in product defects. Alternatively if the evaporation process is too slow, the ink may not densify, ultimately causing an increase in resistance. A balance in applied energy and time must be struck in any given sintering process, which often times leads to a bottle neck.

Additionally, the high temperatures needed for conventional sintering limits the types of substrates that can be used in printing. If the temperatures used are well below the melting temperatures of the bulk metal, the metal remains in the solid state. Considering that the metal nano particles are contained within the binder of the ink, only limited mass transfer along the substrate/ink interface is available for the metal nano particles. This results in a reduction of conductivity when compared to the bulk metal.

A breakthrough curing/sintering method was presented in K. A. Schroder, et al. (2006). The breakthrough sintering method, known as photonic sintering, offers the very specific advantage of rapidly heating the thin ink film created during the printing process while the remainder of the substrate remains cool. This is achieved by a broadcasted

International Journal of Engineering Research & Technology (IJERT)
ISSN: 2278-0181
Vol. 5 Issue 03, March-2016

pulse of high intensity light from a xenon bulb. Nano particles are usually thermally absorbing bodies of high surface area to mass ratio. As a result, little light is needed to heat the particles. With this system, heat is transferred to the ink film within milliseconds. The key difference between photonic vs conventional sintering is that photonic sintering emits an intense enough light that thermal equilibrium between particles and substrate is never achieved. The result is the particles are sintered then cooled before any substantial heat transfer to the substrate occurs [11].

The photonic curing equipment used was a Pulse Forge 1200 manufactured by Novacentrix, Austin, TX. It utilizes a water cooled xenon lamp, capable of producing energies of up to 21 J/cm^2. The machine utilizes a software interface called Pulse Forge. Pulse Forge allows for the changing of key parameters that affect the sintering process. These sintering parameters are:

1. Voltage – The voltage supplied to the sintering lamp.
2. Envelope Duration – Total time for a set of micro pulses used to photonically sinter the chosen sample, and the rest time between pulses.
3. µ Pulses – The number of pulses of light from the lamp.
4. Duty Cycle – The ratio of time the flash lamp is on to the time the flash lamp is off.

In addition to these machine settings, the motion of the specimen during the lamp operation can be changed to accommodate (once through) web speeds of up to 6.1 m/min. During operation, the specimen and stage move directly under the sintering lamp. The lamp then discharges a particular predetermined amount of stored electromagnetic energy, which is absorbed by the specimen. The discharge rate can be varied by changing a machine parameter entitled "fixed position".

D. Quality Testing

1) Design of Experiment

The design of experiment (DOE) is a combination of two 2^2 full factorial designs. Each was such that the adhesive characteristics and resistivity of the silver nano ink films printed on ITO coated glass specimens with and without adhesion promoting glass frit (VS1307) can be analyzed for 2 different sets of sintering parameters. The first experiment investigated adhesion and resistivity of specimens with and without the (VS1307), and a relatively high amount of energy (mJ/cm^2) and a relatively low amount of energy. These conditions are represented by +1, -1, E+1 and E-1 in Experiment 1, of

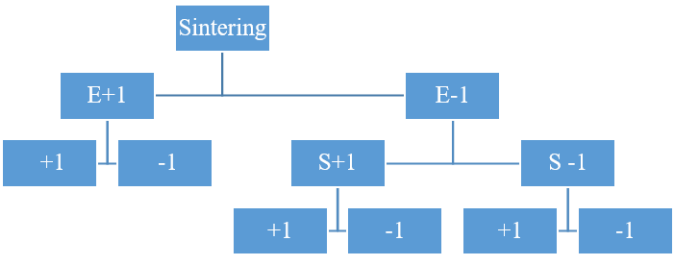

Fig. 4, respectively. The second experiment investigated adhesion and resistivity of specimens with and without VS1307, at a relatively fast sintering speed (ft/min), and relatively slow sintering speed, These factors are represented by +1, -1, S+1, S-1 in Experiment 2, of

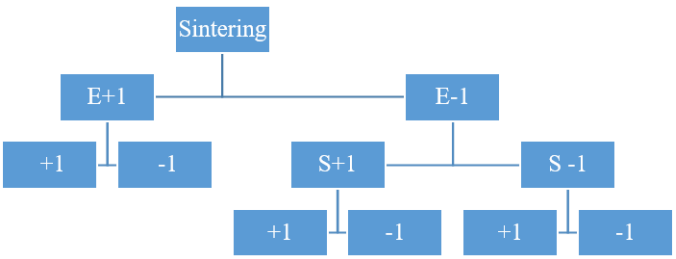

Fig. 4, respectively.

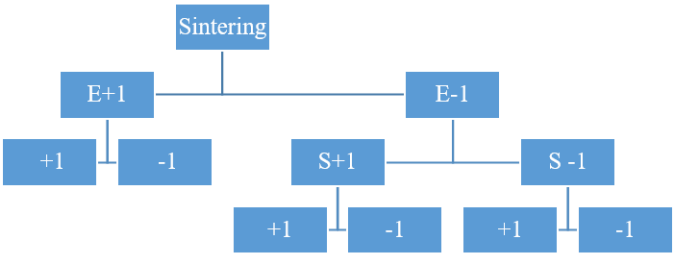

Fig. 4. Design of Experiment Mapping Chart.

Table 1 is a summary of the sintering profiles and the associated parameters. Not included in Table 1 is the distance between stage and flash lamp, which was held at 20 mm for all tests.

International Journal of Engineering Research & Technology (IJERT)
ISSN: 2278-0181
Vol. 5 Issue 03, March-2016

Table 1. Sintering Profiles for Novacentrix PulseForge 1200 Used for Proof of Concept.

DOE Factors	Voltage	Pulse Length	No. of μ-pulses	Envelope	Duty Cycle	Mode	Stage Speed	Energy
Energy / Speed	Volts	ms	n/a	n/a	n/a	n/a	ft/min	mJ/cm^2
E+1 / S-1	440	9000	1	10000	0.90	once through	5	14130
E-1 / S-1	330	450	1	500	0.90	once through	5	900
E-1 / S+1	330	450	1	500	0.90	once through	20	900

2) Adhesion

Adhesion can be theoretically modeled by means of the Young's Modulus, but given the complexities of the adhesion process, it is reasonable to state that presently no test can precisely assess the actual physical strength of an adhesive bond. There is, however, a way to obtain an indication of relative adhesion performance [12], [13]. For this reason, currently practiced industry standards were considered to provide a method of measuring adhesion. Quantifying adhesive characteristics based on the force needed to remove the film from the substrate was determined by measuring the film's resistance to abrasion. The procedure followed was adapted from Technical Association of the Pulp and Paper (TAPPI) T-467 standard test method, utilizing a Taber 5130 Abraser, manufactured by Taber, North Tonawanda, NY.

The Taber 5130 is a device that rotates a specimen resting on a turntable on a central vertical axis, while applying an abrasive force via 2 abrasive discs (CS-10 Calibrase Wheels) that also rotate on a perpendicular axis. The axis of rotation of the abrasive wheels is displaced from that of the turntable creating an abrasive "sliding" action as the specimen rotates. Fig. 5 is an illustration of the abrasive action utilized by the Taber 5130. The abrasive wheel provided a wear area of 300 mm^2. The applied force to the Calibrase Wheels was 0.25 N. The turntable rotated at 72 revolutions per minute [14].

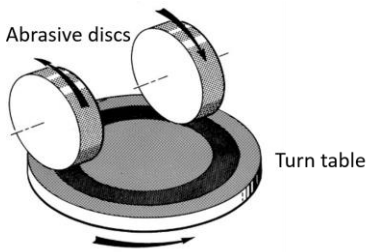

Fig. 5. Abrasion Action Utilized by Taber 5130 [15].

The TAPPI T-476 standard outlines a test for the resistance of surface to the act of abrasion. The way to quantify this is by a mass method. The mass of the specimen is measured before and after being subjected to the abrasive wheels, and is then compared to provide a relative measure of the film's adhesion [15]. This was not chosen due to variation in the registration of subsequent layers (Fig. 6). Small variation in the position of each layer in reference to one another creates variation in area subjected to the abrasive wheels, thus an alternate method was needed.

The number of revolutions was fixed at five, which provided enough abrasion such that both the remaining printed film and the ITO coated glass substrate was visible to the naked eye. The partial exposure of the substrate could then be analyzed.

The method used to analyze the partial exposure of glass of each specimen was achieved with software and a camera-based solution developed by ImageXpert, Nashua, NH. The software is an automated visual system that evaluates changes from light pixels to dark along a grey scale ranging from 0 (black) to 255 (white). The software utilizes an algorithm to calculate the percentage of area still covered by the printed film. The threshold, or grey value that divides light pixels from dark pixels, was determined by placing a specimen at the edge of glass substrate and printed film, then adjusting the grey value until there is a clear distinction between glass and printed film. Fig. 7 illustrates the appropriate threshold, with the top half representing the bare glass, and the lower half representing the untouched printed film. The inclusion of the histogram in Fig. 7 shows at what gray tone represents the bare glass. Fig. 8 is an example of the type of comparison of specimens post abrasion as analyzed by the Image Expert software for the Percent glass exposed. Fig. 8. A. illustrates a specimen with low percent film, relative to that of the specimen in Fig. 8. B. The greater the percent film that has been removed from the abrasion test, the greater the number of light pixels (top half of Fig. 7).

For each specimen, nine random regions of interest (ROI) were chosen for analysis. The ROI was 640-480 pixels and positioned within the abraded area. Fig. 6 illustrates an example of the ROI and other features of any given specimen.

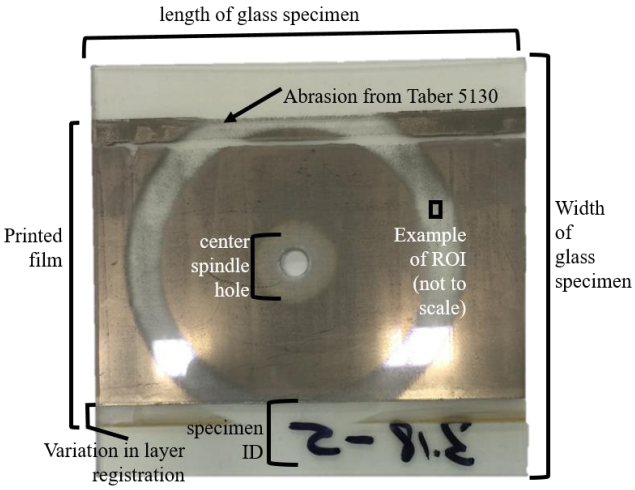

Fig. 6. Sample Diagram of Taber Test Specimen.

International Journal of Engineering Research & Technology (IJERT)
ISSN: 2278-0181
Vol. 5 Issue 03, March-2016

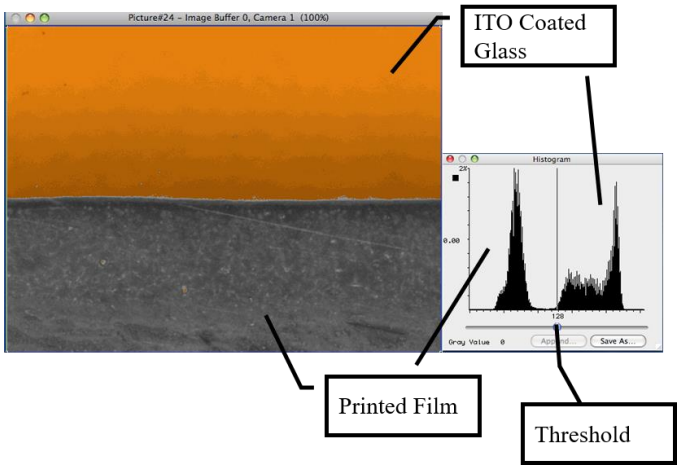

Fig. 7. ImageXperts Analysis: Determining Glass from Printed Film.

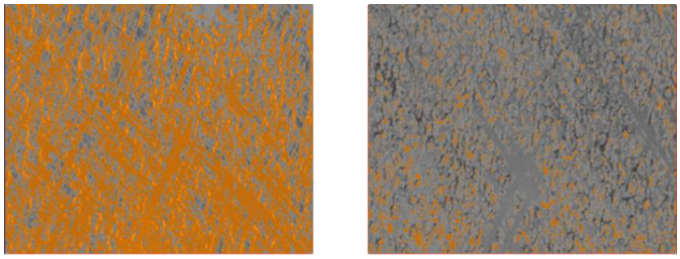

A B

Fig. 8. Comparison of Specimens Post Abrasion Analyzed by Image Expert Software for Percent Glass Exposed.

3) Resistance

Resistivity of the printed film/substrate was determined through the use of a Keithley 2400 Source Meter. The mean of 9 readings, taken in a grid pattern as shown in Fig. 9, was used obtain the resistivity measurement of each specimen. The grid spacing was approximately 2 cm in both directions. The total film dimensions were on approximately 7 x 11 cm.

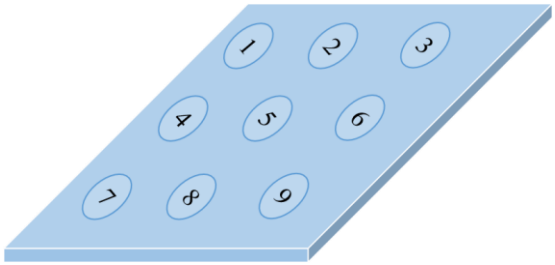

Fig. 9. Schematic for Average Resistivity Measurement

III. RESULTS

Prior to adhesion and resistivity testing, scanning electron microscopy images were taken to qualify the differences in adhesion and resistivity.

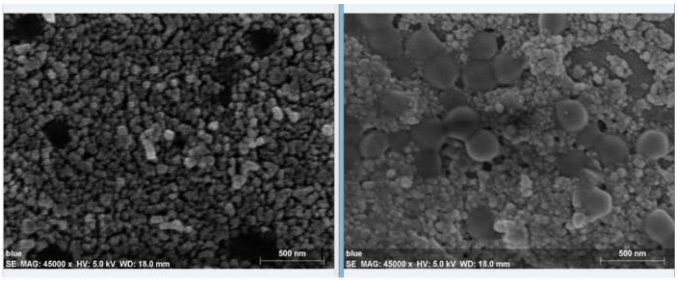

A B

Fig. 10. A is the printed silver nano ink film printed on ITO coated glass, and

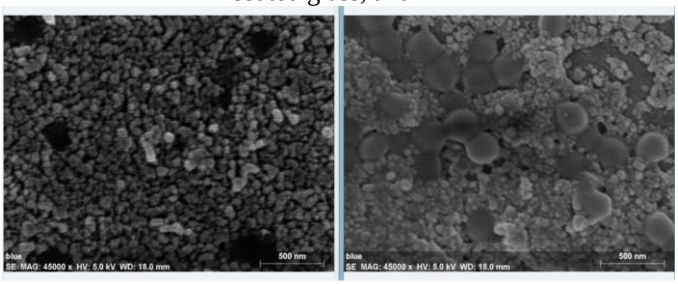

A B

Fig. *10*.B is the same printed silver nano ink film on ITO, but with the addition of a VS1307 layer. VS1307 is evident in the sample by the presence of larger glass frit particles. A comparison of the processed VS1307 (i.e., printed and sintered) with that of VS1307 in its raw form, as presented in

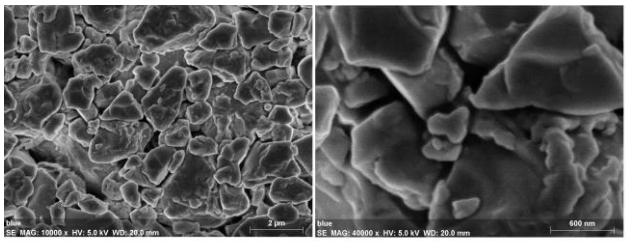

A B

Fig.2. The images clearly show that enough energy was applied during the sintering process to melt the glass frit particles. This is evident by the size reduction and deformation of the particles.

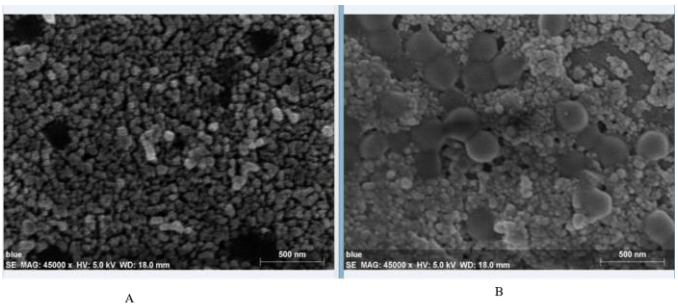

A B

Fig. 10. Scanning Electron Microscope image of (A) without VS1307 and (B) with VS1307.

International Journal of Engineering Research & Technology (IJERT)
ISSN: 2278-0181
Vol. 5 Issue 03, March-2016

Comparison of the two images in

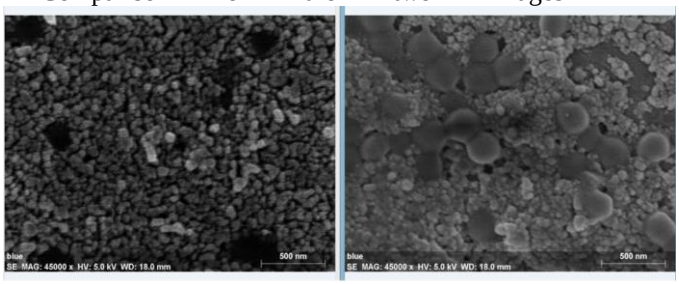

Fig. *10* clearly shows there is a decrease in the number of voids in the presence of VS1307. This densification of the sintered film is in agreement with the results obtained by Jang, et al. (2008). The key difference between the two is the method by which they were sintered. Jang used a conventional thermal chamber heated to sintering temperatures, while here the ink was sintered by means of photonic energy.

Model adequacy must always first be considered. It is assumed that the error embedded in the experiment is normally distributed, which becomes important when performing analysis of variance for the data. Departures from normality usually causes the significance level of the factors, i.e., sintering parameters and presence of VS1307 to differ from advertised values. Significance for effects studied in this experiment was based on an F-test.

A check of the normality assumption was made by constructing a normal probability plot using Minitab® Statistical Software. The plot is constructed by plotting the residuals against the normal percent probability. The residuals, or the amount of variability in a dependent variable that remains after accounting for the variability attributed to any predictors in the analysis, resulted from the percent film remaining after subjugation to the Taber abrasion test and resistance measured by four point collinear probe. Fig. 11 shows that the error distribution is for the adhesion portion of Experiment 1 approximately normal as evident by the concentration of the residual data near the 50% mark and that they are approximately linear [16]. Adhesion and resistivity for Experiment 1 and 2 follow the normality assumption.

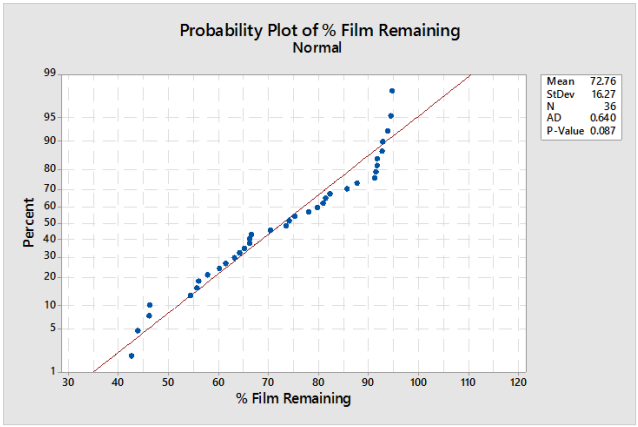

Fig. 11. Normal Probability Plots for Adhesion of Experiment 1.

A. *Adhesion*

For analysis of the DOE the hypothesis and null hypothesis respectively was as follows: The percent film remaining is dependent on energy or presence of frit, and the percent film remaining is not dependent on energy or presence of frit, respectively. All means present throughout the study are data means and not fitted means.

Two trends emerge after analyzing the results of the Experiment. Trend 1 is the average percentage of film remaining on the substrate after the Taber abrasion test is approximately 9.5% greater when the layer of frit was included. Trend 2 is that the increase from 900 mJ/cm^2 to 14130 mJ/cm^2 of energy applied during the photonic sintering process increases the percent of film remaining by approximately 20%.

Fig. 12 is a main effects plot that illustrates trends 1 and 2. This plot compares side by side the effect of each factor has on the percent film remaining on the substrate. From this plot, one can easily see that of the given choices, the desired settings of +1 and E+1 should be chosen to provide a greater percentage of film remaining, or greater adhesive strength of the film.

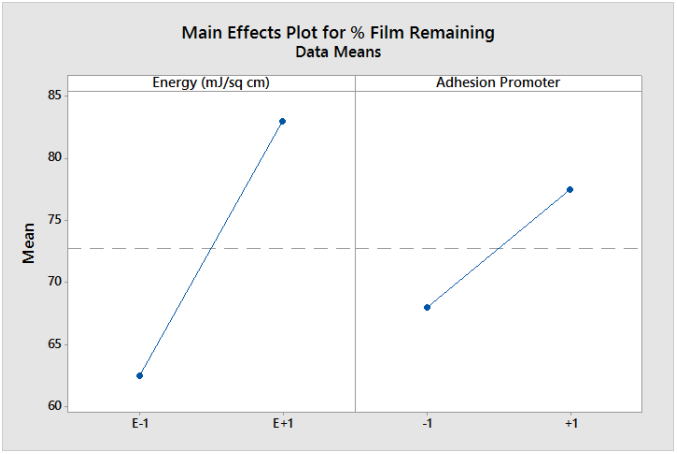

Fig. 12. Main Effect Plot for Percent Film Remaining on Substrate for Experiment 1.

A determination of standardized effects was made for energy, the presence of the adhesion promoter (frit) and a possible interaction between the two using a significance level (α) of 0.05.

Fig. *13* illustrates this using a standardized effect plot. The model used for all main effects plots was the General Full Factorial.

The statistical significance of the factors was based upon evaluation of the p-value, or probability of obtaining a test statistic at least as extreme as the one actually calculated from the sample, if the null hypothesis is true. The p-value for the hypothesis is such that it is too unlikely to have occurred by chance [17]. The interaction between energy and frit is however not statistically significant.

Fig. *13* illustrates the energy is most statistically significant, as it has the greatest magnitude on the standardized effects scale.

International Journal of Engineering Research & Technology (IJERT)
ISSN: 2278-0181
Vol. 5 Issue 03, March-2016

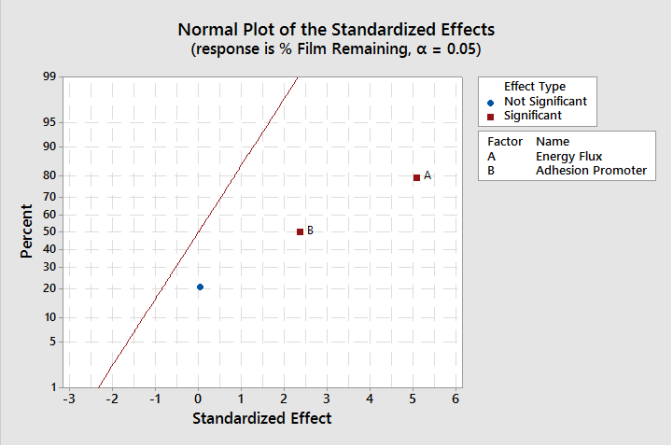

Fig. 13. Normal Plot of the Standard Effects for Percent Film Remaining for Experiment 1.

Experiment 2 varied sintering speed and the presence of frit. Experiment 2 proved an approximate 30% increase in percent film remaining on substrate occurred for a decrease in sintering speed.

As with Experiment 1, the main effects of Experiment 2 were analyzed as they relate to percent film remaining. As dictated by Experiment 2 of the DOE, the effects of stage speed and presence of the adhesion promoting glass frit are compared. From Fig. 14 the percent of film remaining would be greatest if the sintering was done with a slower stage speed. It would seem that according to Fig. 14 there is a slight increase in the percent film remaining should a layer of frit be present. However, analysis of standardized effects, (Fig. 15), suggests that for Experiment 2, presence of frit or the frit's interaction with sintering speed does not have statistical significance as a standardized effect.

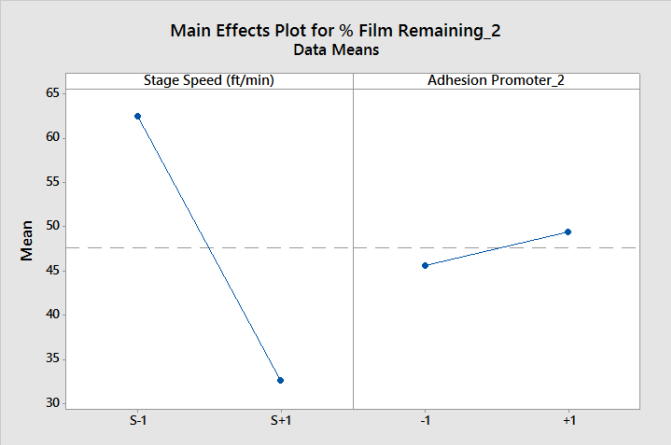

Fig. 14. Main Effect Plot for Percent Film Remaining on Substrate for Experiment 2.

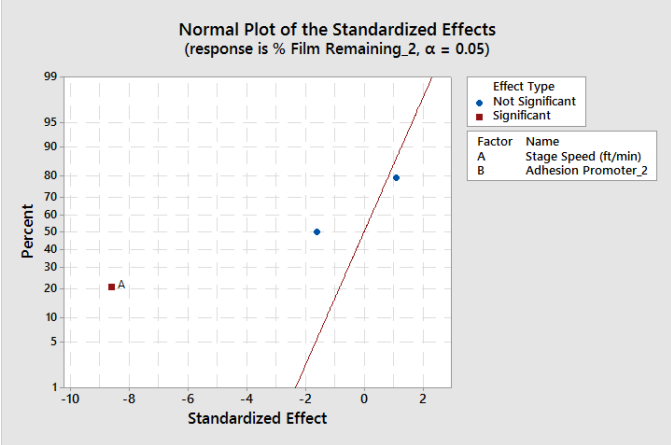

Fig. 15 Normal Plot of the Standard Effects for Percent Film Remaining for Experiment 2.

This contradicts the results of Experiment 1, in which the adhesion promoter was a standardized effect that is statistically significant. One theory for why the effect of the frit would differ between experiments is that with the increased sintering speed, insufficient energy is absorbed by the frit to sinter to adjacent frit and/or silver nano particles. Additional testing to confirm this theory is recommended.

B. Resistivity

Resistivity for experiment 1 and 2 was analyzed in similar fashion to experiment 1 and 2 for adhesion. The hypothesis is film resistance is dependent on sintering speed or presence of frit. The null hypothesis is film resistance is not dependent on sintering speed or presence of frit.

Considering Experiment 1, an increase in film resistance was exhibited for a decrease energy applied during the sintering process. Specimens sintered with an energy of 900 mJ/cm^2 presented on average 37 times higher resistivity than specimens sintered with 14130 mJ/cm^2. This is a dramatic increase and is consistent with sintering theory. The greater the energy applied by the xenon light source, the greater the amount of energy absorbed by the silver nano particles, which results in greater surface area for contact after melting, and consequently, lower the resistivity. Fig. 16 is a graphical representation of Experiment 1 as it relates to resistance, and includes the aforementioned energy/resistance relationship. It is important to note that resistance of the bare ITO coated glass was measured and was on average 2.75 Ω/sq., which shows conductive functionallity of all printed film, regardless of the presence of frit.

When looking at the associated main effects plot for resistivity as a function of energy and glass frit the advantagous parameter for ensuring the lowest possible resistance is higher energy. Fig. 16 also shows that addition of the frit layer can work to reduce film sheet resistance, but further analysis goes to show that presence of the frit layer is not statistically significant. Fig. 17 shows this with a normal plot of the standard effects.

International Journal of Engineering Research & Technology (IJERT)
ISSN: 2278-0181
Vol. 5 Issue 03, March-2016

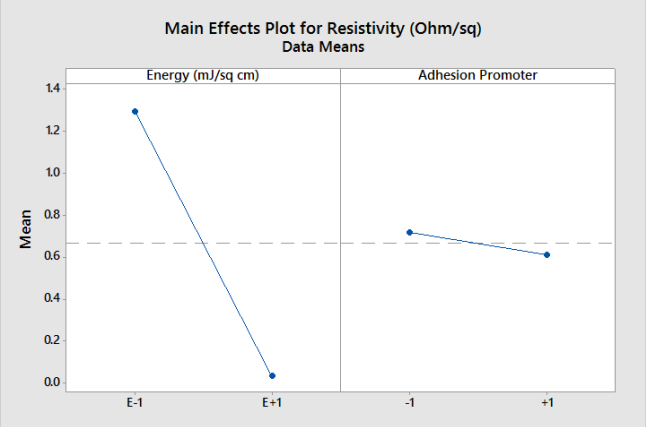

Fig. 16. Main Effect Plot of Film Resistance for Experiment 1.

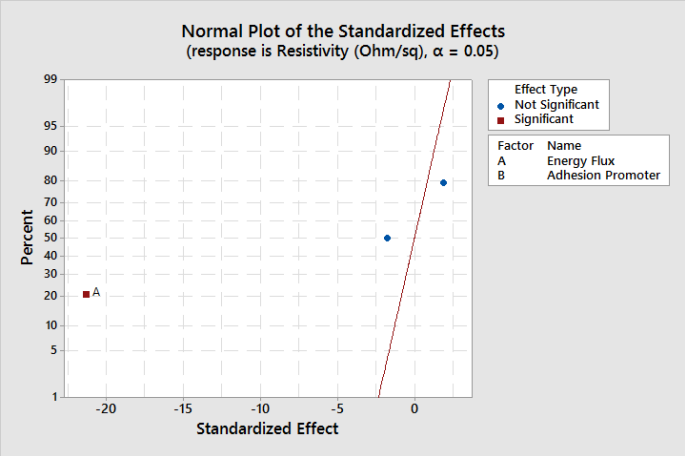

Fig. 17. Normal Plot of the Standard Effects on Film Resistance for Experiment 1.

No clear trend(s) emerge when analyzing film resistance as a function of sintering speed, with and without frit. For both sintering speeds (5 and 20 ft/min) and whether the frit layer is present, film resistivity remains relatively close to a median of 1.24 ohms/sq, with a standard deviation of 0.46 ohms/sq. This would seem contrary to the main effects, and normal standardized effects plots, (

Fig. *18*, and Fig. 19 respectively). These plots show that there is a desirable set of parameters, and that both sintering speed and the frit presence is statistically significant. However, what Fig. 19 also illustrates the interaction between sintering speed and frit is also statistically significant and is the dominating effect.

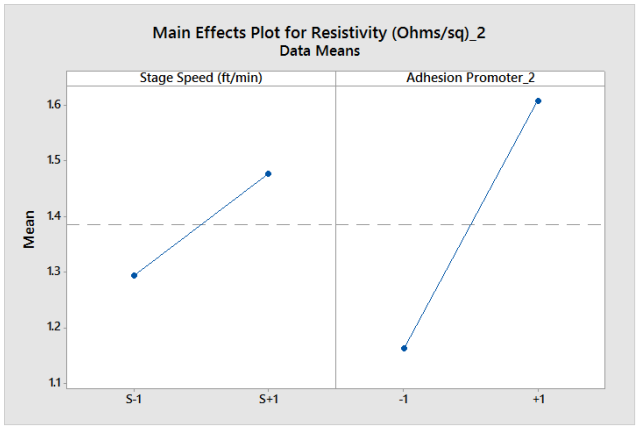

Fig. 18. Main Effect Plot of Film Resistance for Experiment 2.

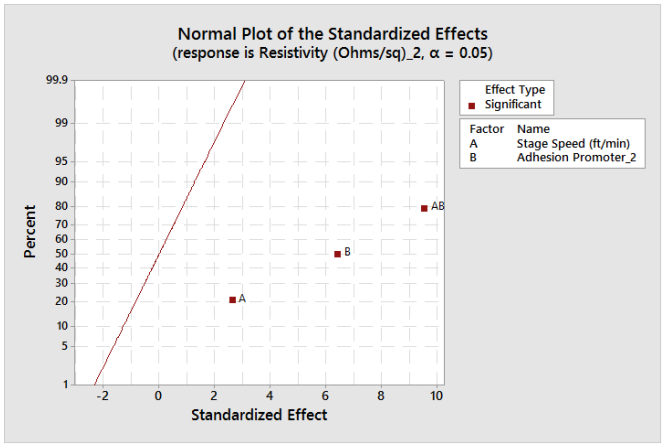

Fig. 19. Normal Plot of the Standard Effects on Film Resistance for Experiment 2.

To analyze further, an interaction plot was generated, (

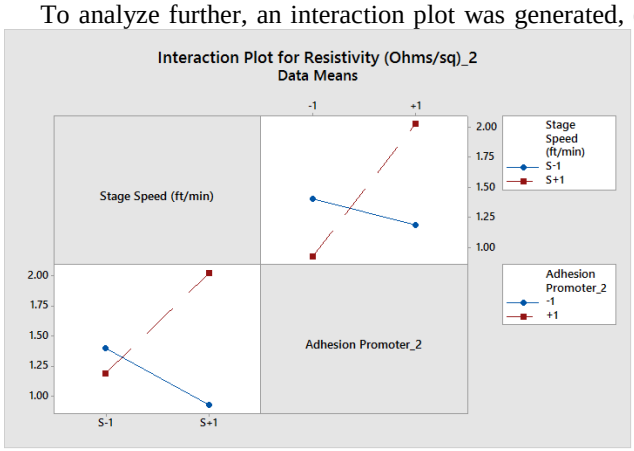

Fig. *20*), in order to break into smaller components the effects of each variable. An interaction plot is a plot of means for each level of a factor with the level of a second factor held constant. The greater the deviation from parallel lines, the greater the degree of interaction, and the intersecting lines in

International Journal of Engineering Research & Technology (IJERT)
ISSN: 2278-0181
Vol. 5 Issue 03, March-2016

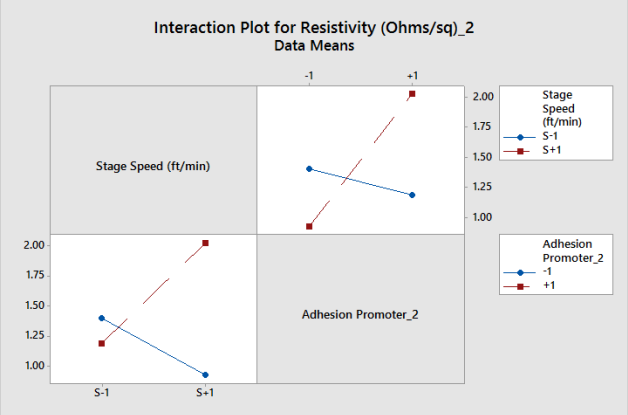

Fig. *20* represents a strong interaction between the two factors [18]. The top right quadrant of

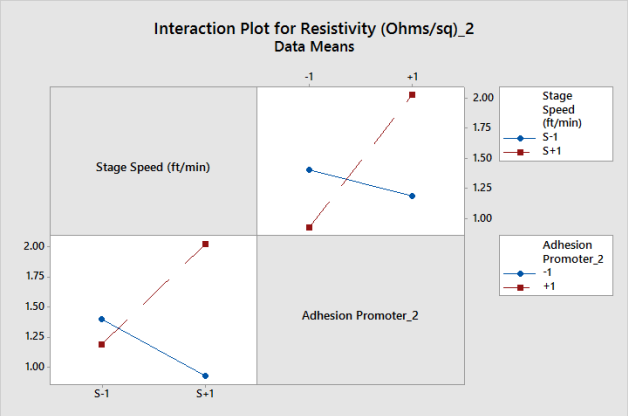

Fig. *20* shows that for S+1 resistivity decreases if a frit layer is present. It also shows that for S-1, resistivity increases less dramatically if a frit layer is present. The bottom left quadrant shows that for -1 resistance decreases with increasing sintering speed. The bottom left quadrant also shows that for +1 an increase in resistance for an increase in sintering speed. Considering both quadrants, a coveted low resistance could be facilitated by a fast sintering speed, (S+1) with frit (-1). This setup for optimum resistance has the opposite sintering speed as that of the optimum adhesion setup, frit is desired in both resistance and adhesion optimization.

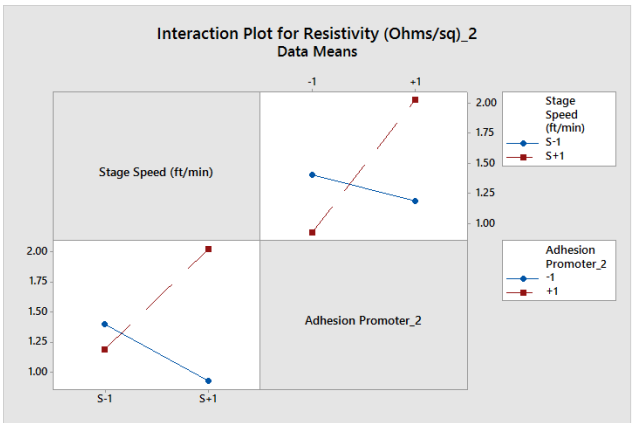

Fig. 20. Interaction Plot of Sintering Speed and Adhesion Promoting Frit for Film Resistivity.

IV. CONCLUSIONS

A process to produce a printed conductive film on ITO coated glass was demonstrated using a photonic sintering/curing method. A conductive film was printed using silver nano particle ink and flexography onto an ITO coated substrate, then sintered using Novacentrix PulseForge 1200. An adhesion promoting layer containing 27–33% low melting glass frit was printed using the same flexographic printing method to study its effect on adhesion and resistance. The adhesion was studied using a novel method that utilizes the combination of mechanical abrasion and pixel analysis software. Resistance was studied with the aid of a four point collinear probe.

Adhesion improved with an increase in energy, and presence of frit, for which both factors were statistically significant. Adhesion decreased with an increase in sintering speed. Resistivity decreased dramatically for an increase in energy applied and the presence of the adhesion promoter had no significant effect. A clear trend for resistivity as a function of sintering speed was not observed.

V. REFERENCES

[1] J. Perelaer, P. J. Smith, D. Mager, D. Soltman, S. K. Volkman, V. Subramanian, J. G. Korvink and U. S. Schubert, "Printed eletronics: the challenges involved in printing devices, interconnects and contacts based on inorganic materials," *Journal of Materials Chemistry*, vol. 1, no. 20, pp. 8446-8453, 2010.

[2] K. Suganuma, Introduction to Printed Electronics, New York: Springer, 2014.

[3] E. Broitman, "What is the best way to promote adhesion between glass and chromium?," Unpublished, 2013. [Online]. Available: http://www.researchgate.net/post/What_is_the_best_way_to_promote_adhesion_between_glass_and_chromium. [Accessed 30th April 2014].

[4] B. Kanegsberg and E. Kanegsberg, Handbook for Critical Cleaning, Portland, Oregon: CRC Press, 2001.

[5] D. Jang, D. Kim, B. Lee, S. Kim, M. Kang, D. Min and J. Moon, "Nanosized glass frit as an adhesion promoter for ink-jet printed conductive patterns on glass substrates annealed at high temperatures," *Journal of Advanced Functional Materials*, vol. 18, pp. 2862-2868, 2008.

[6] Hitachi Chemical Co. , *Safety Data Sheet VS-1307*, Katori-Gun, Chiba, 2014.

[7] in *Center for the Advancement of Printed Electronics Free Flexible Electronics Networking Event*, Kalamazoo, 2014.

[8] K. Sivaramakrishnan, A. T. Ngo, S. Iyer and T. L. Alford, "Effect of thermal processing on silver thin films of varying thickness deposited on zinc oxide indium tin oxide," *Journal of Applied Physics*, vol. 105, 2009.

[9] Haper Scientific, "QD Proofing System," Harper Scientific, 2015. [Online]. Available: http://www.harperimage.com/HarperScientific/Phantom-QD/product-25. [Accessed 1 June 2015].

[10] J. West, M. Carter, S. Smith and J. Sears, "Photonic Sintering of Silver Nanoparticles: Comparison of Experiment and Theory," in *Sintering - Methods and Products*, Rijeka, InTech, 2012, pp. 173-188.

[11] K. A. Schroder, S. C. McCool and W. F. Furlan, "Broadcast photonic curing of metallic nanoparticle films," in *The 2006 NSTI Nanotechnology Conference and Trade Show*, 2006.

[12] K. L. Mittal, ""Adhesion measurement: recent progress, unsolved problems, and prospects," adhesion measurement of thin films, thick films, and bulk coatings," *ASTM*, vol. ATSM STP 640, pp. 7-8, 1978.

International Journal of Engineering Research & Technology (IJERT)
ISSN: 2278-0181
Vol. 5 Issue 03, March-2016

[13] K. L. Mittal, "Smposium on Adhesion Aspects of Polymeric Coatings," in *Proceedings, The /Electrochemical Society*, 1981.
[14] Taber Industries, "Taber Abraser 5130/5150," [Online]. Available: http://www.ccsi-inc.com/taberabraser_5130_5150.pdf. [Accessed 20 June 2015].
[15] "TAPPI T-467".
[16] D. C. Montgomery, Design and Analysis of Experiments, 8th ed., Hoboken, New Jersey: John Wiley & Sons, Inc, 2013, pp. 80-81.
[17] Minitab Inc., ""Minitab Statistical Glossary", Statistical Significance," 2010.
[18] Minitab Inc, ""Minitab Statistical Glossary," Interaction Plots," 2010.
[19] ASTM Standard D 3359-09ε2, "Standard Test Methods for Measuring Adhesion by Tape Test," *ASTM International*, p. DOI:23, 2009.
[20] N. Chivoranund, S. Jiemsirilers and D. P. Kashima, "Effects of surface treatments on adhesion of silver film on glass substrate fabricated by electroless plating," *Journal of the Australian Ceramic Society*, vol. 49, no. 1, pp. 62-69, 2013.
[21] M. J. Guillot, K. A. Schroder and S. C. McCool, "Simulating the thermal response of thin films during photonic curing," in *Proceedings of the ASME 2012 International Mechanical Engineering Congress & Exposition*, Houston, 2012.
[22] S. Mahdi, "Organic/inorganic coatings cured by ultraviolet light and moisture for automotive glass," *SAE International*, vol. 5, no. 2, pp. 499-502, 2012.